16, or 32) and PS-*dendr*-$(\mathrm{NH_2})_n$ (n = 2, 4, 8, 16, or 32) was performed with ^{1}H NMR, ^{13}C NMR, and infrared spectroscopy. For example, PS-*dendr*-$(\mathrm{CN})_{32}$: ^{1}H NMR ($\mathrm{CDCl_3}$) chemical shift δ 0.54 to 0.78 [br, 6H, $\mathrm{C\underline{H}_3\text{-}CH_2\text{-}CH(C\underline{H}_3)\text{-}(CH_2\text{-}CHPh)}_n$ (Ph, phenyl)], 0.78 to 2.74 ($\mathrm{CH_3\text{-}C\underline{H}_2\text{-}C\underline{H}(CH_3)\text{-}(C\underline{H}_2\text{-}C\underline{H}Ph)}_n\mathrm{\text{-}CH_2\text{-}O\text{-}CH_2\text{-}CH_2\text{-}CH_2\text{-}N}$), 1.52 to 1.68 (br, 60H, $\mathrm{N\text{-}CH_2\text{-}C\underline{H}_2\text{-}CH_2\text{-}N}$), 2.30 to 2.62 (br, 122H, $\mathrm{O\text{-}CH_2\text{-}CH_2\text{-}C\underline{H}_2\text{-}N}$ + $\mathrm{N\text{-}CH_2\text{-}CH_2\text{-}C\underline{H}_2\text{-}N}$), 2.45 (t, J = 6.6 Hz, 64H, $\mathrm{N\text{-}CH_2\text{-}C\underline{H}_2\text{-}CN}$), 2.82 (t, J = 6.6 Hz, 64H, $\mathrm{N\text{-}C\underline{H}_2\text{-}CH_2\text{-}CN}$), 3.13 to 3.45 (br, 4H, $\mathrm{CH_2\text{-}CHPh\text{-}C\underline{H}_2\text{-}O\text{-}C\underline{H}_2\text{-}CH_2\text{-}CH_2\text{-}N}$), 6.25 to 7.32 [$\mathrm{(CH_2\text{-}CH\underline{Ph})}_n$]; ^{13}C NMR ($\mathrm{CDCl_3}$) δ 11.0 to 11.4 [br, $\mathrm{\underline{C}H_3\text{-}CH_2\text{-}CH(CH_3)\text{-}(CH_2\text{-}CHPh)}_n$], 16.8 (32x, $\mathrm{N\text{-}CH_2\text{-}\underline{C}H_2\text{-}CN}$), 18.8 to 20.0 [br, $\mathrm{CH_3\text{-}CH_2\text{-}CH(\underline{C}H_3)\text{-}(CH_2\text{-}CHPh)}_n$], 23.7 (2C+4C+8C, $\mathrm{N\text{-}CH_2\text{-}\underline{C}H_2\text{-}CH_2\text{-}N}$), 24.6 (16C, $\mathrm{N\text{-}CH_2\text{-}\underline{C}H_2\text{-}CH_2\text{-}N}$), 26.5 (1C, $\mathrm{O\text{-}CH_2\text{-}\underline{C}H_2\text{-}CH_2\text{-}N}$), 28.1 to 30.2 [br, $\mathrm{CH_3\text{-}\underline{C}H_2\text{-}CH(CH_3)\text{-}(CH_2\text{-}CHPh)}_n$], 31.3 [$\mathrm{CH_3\text{-}CH_2\text{-}\underline{C}H\text{-}(CH_3)\text{-}(CH_2\text{-}CHPh)}_n$], 40.1 [$\mathrm{CH_3\text{-}CH_2\text{-}CH(CH_3)\text{-}(CH_2\text{-}\underline{C}HPh)}_n$], 39.8 to 46.6 [br, $\mathrm{CH_3\text{-}CH_2\text{-}CH(CH_3)\text{-}(\underline{C}H_2\text{-}CHPh)}_n$], 49.0 (32C, $\mathrm{N\text{-}\underline{C}H_2\text{-}CH_2\text{-}CN}$), 52.0 to 50.4 (br, 1C, $\mathrm{O\text{-}CH_2\text{-}CH_2\text{-}\underline{C}H_2\text{-}N}$, 2C+2C+4C+4C+8C+8C+16C+16C, $\mathrm{N\text{-}\underline{C}H_2\text{-}CH_2\text{-}\underline{C}H_2\text{-}N}$), 69.6 to 69.2 [br, $\mathrm{(CH_2\text{-}CHPh)}_n\mathrm{\text{-}CH_2\text{-}O\text{-}\underline{C}H_2\text{-}CH_2\text{-}CH_2\text{-}N}$], 75.2 to 76.2 [br, $\mathrm{(CH_2\text{-}CHPh)}_n\mathrm{\text{-}\underline{C}H_2\text{-}O\text{-}CH_2\text{-}CH_2\text{-}CH_2\text{-}N}$], 118.7 (32C, $\mathrm{\underline{C}N}$), 125.2 to 127.0 (br, $\mathrm{CH_2\text{-}CH\underline{Ph}}_{para}$), 127.1 to 130.0 (br, $\mathrm{CH_2\text{-}CH\underline{Ph}}_{ortho+meta}$), 145.1 to 146.6 (br, $\mathrm{CH_2\text{-}CH\underline{Ph}}_{ipso}$); IR: frequency $\nu_{\mathrm{C\equiv N}}$, 2246 $\mathrm{cm^{-1}}$.

13. The dendrimer part is confined in space, but a variety of PS chain conformations is possible; we show an extended chain, similar to the representations of traditional surfactants.
14. The aqueous aggregates were prepared according to the following procedure: the amphiphiles were dissolved in 2 ml of toluene or tetrahydrofuran. After the addition of 25 ml of water, the organic solvents were evaporated and stable aggregates were formed. The PS-*dendr*-$(\mathrm{NH_2})_{32}$ system even gave a clear solution in water, thereby indicating a remarkably low Krafft temperature for this structure.
15. The observed vesicular structures show a resemblance to the structure proposed by Kunitake *et al.* [T. Kunitake, N. Kimizuka, N. Higashi, N. Nakashima, *J. Am. Chem. Soc.* **106**, 1978 (1984); T. Kunitake, M. Nagai, H. Yanagi, K. Takarabe, N. Nakashima, *J. Macromol. Sci. Chem.* **21** (no. 8–9), 1237 (1984)].
16. For the techniques used to observe spherical micelles with TEM, see O. Regev, C. Kang, A. Khan, *J. Phys. Chem.* **98**, 6619 (1994).
17. We thank E. M. M. de Brabander-van den Berg for discussions on dendrimer synthesis; J. Joosten and A. Moussaid for performing the DLS measurements; H. van Nunen, H. Geurts, and Y. Engelen for assistance with the TEM measurements; and A. van Kraay for the molecular modeling. This research was supported under a DSM Research unrestricted research grant.

4 January 1995; accepted 28 March 1995

EUVE Observations of Jupiter During the Impact of Comet Shoemaker-Levy 9

G. Randall Gladstone, Doyle T. Hall, J. Hunter Waite Jr.

The Extreme Ultraviolet Explorer (EUVE) satellite conducted extensive observations of the jovian system before, during, and after the impact of the fragments of comet Shoemaker-Levy 9 in July 1994. About 2 to 4 hours after the impacts of several of the larger fragments, the brightness of the neutral helium (He I) resonance line at 58.4 nanometers temporarily increased by a factor of about 10. The transient 58.4-nanometer brightenings are most simply explained by resonant scattering of sunlight from the widespread high-altitude remnants of the larger impact plumes. Other possible sources of emission, such as electron impact excitation of He or radiative recombination of He^{+}, may contribute to the observed signal.

Observations of extreme ultraviolet (EUV) emissions from the neutral helium resonance line at 58.4 nm were recognized years ago as an excellent means for studying the upper atmosphere of Jupiter (*1*). The He I 58.4-nm line on Jupiter is principally excited by resonant scattering of sunlight (*2*), and its brightness depends primarily on the relative abundances of helium and hydrogen in the jovian upper atmosphere. Both molecular and atomic hydrogen are strong absorbers of 58.4-nm radiation; because they are both lighter than helium, their relative abundances increase in the region above the well-mixed part of the atmosphere, and the probability of absorption for a 58.4-nm photon increases likewise. The altitude separating the well-mixed lower region of the atmosphere (where all long-lived species share a common altitude dependence or scale height) from the diffusive-equilibrium upper atmosphere (where each long-lived species has a different scale height, according to mass) is known as the homopause. The homopause level depends on upper atmosphere dynamics. With vigorous circulation, the homopause will be at high altitude; with more sluggish circulation, it will drop to a lower altitude. Through absorption by the overlying column of H and H_2, the brightness of the He I 58.4-nm emission on Jupiter provides a direct indication of the altitude of the homopause and thus provides information about the dynamics of the jovian upper atmosphere. The strength of the solar He I 58.4-nm line (*3*) and the chemical inactivity of helium (*4*) make the 58.4-nm brightness an ideal diagnostic of vertical mixing in the upper atmospheres of the giant planets.

G. R. Gladstone and J. H. Waite Jr., Department of Space Sciences, Southwest Research Institute, 6220 Culebra Road, San Antonio, TX 78228, USA.
D. T. Hall, Center for Astrophysical Sciences, Department of Physics and Astronomy, Johns Hopkins University, Baltimore, MD 21218, USA.

The Pioneer 10 EUV photometer measured a 5.1-rayleigh (R) (*5*) signal in late 1973 that was attributed to the He I 58.4-nm feature (*6*), although in retrospect, the observation may have been contaminated by EUV emissions from sulfur and oxygen ions in the then unknown Io plasma torus. The ultraviolet spectrometer (UVS) experiments on Voyager 1 and 2 measured He I 58.4-nm brightnesses of 5.2 and 4.4 R, respectively, averaged over much of the dayside disk, during the 1979 encounters (*7*). The brightness differences between the two Voyager UVS measurements are most probably caused by solar cycle variations in the solar He I 58.4-nm line (*3*).

After the Voyager flybys, there were no further observations of EUV emissions from Jupiter until the launch of EUVE in June 1992 (*8*). The EUVE observations are made with three spectrographs that cover a wavelength band from 7.0 to 76.0 nm with a resolving power ($\lambda/\Delta\lambda$) of about 200 to 400 for point sources. The spectrographs share the same grazing-incidence mirror, have circular fields of view about 2° in diameter, and are capable of imaging monochromatic emissions (*9*). For moving sources (such as planets), the photons may be remapped into a target-centered frame of reference by using the arrival times and appropriate ephemerides for the spacecraft and the target (*10*).

Observations of the Jupiter system were made by EUVE in April 1993, and a rich spectrum of the Io plasma torus was obtained. However, no excess He I at 58.4 nm that could have been associated with Jupiter was found (*11*). Observing jovian He I emitting at 58.4 nm is difficult from EUVE's 520-km altitude because of the resonant scattering of sunlight by Earth's extended helium atmosphere or geocorona. The He I 58.4-nm geocoronal foreground emissions are mildly optically thick and depend primarily on solar zenith angle, but they vary rather slowly with look direction at the altitude of EUVE (*12*). The darkest part of the sky to look toward is antisunward at orbital midnight. During EUVE's all-sky survey, this part of the sky was examined routinely for 6 months, from July 1992 until January 1993. A study of the geocoronal brightness in the antisolar direction from 25 July to 19 August 1992 yielded an average brightness of 1.3 R (*13*). In other directions, the 58.4-nm airglow is usually larger. In particular, observations made from within the Earth's shadow at 90° to the Earth-sun line (approximately the geometry during the week of the comet impacts) generally show helium geocoronal airglow brightnesses about twice those in the antisunward direction. The geocoronal He I 58.4-nm brightness was 2.2 R during the April 1993 observations, and the corresponding 2σ upper limit to the He I 58.4-nm brightness from Jupiter was 1.8 R. The decrease since the time of the Voyager measurements is attributed to the variation of solar He I 58.4-nm flux from solar maximum to solar minimum conditions, although changes in the helium abundance of Jupiter's upper atmosphere are also possible. Because previous EUVE searches for a jovian signal at 58.4 nm were negative, we were surprised when the helium showed up strongly in spectral images obtained during the impacts (Fig. 1). The He I 58.4-nm emissions are in fact faintly detectable even before the arrival of the first Shoemaker-Levy 9 fragments. This is probably a result of a decrease in the geocoronal He I 58.4-nm foreground, which dropped from 2.2 R during the April 1993 opposition measurements to about 0.8 R throughout the July 1994 measurements. The enhanced helium emissions clearly originate from the disk of Jupiter, although the low spatial resolution of EUVE limits our ability to investigate the brightness distribution in more detail. By constructing a light curve for 58.4-nm observations, we were able to demonstrate a strong correlation between the enhanced 58.4-nm signal and the times of the fragment impacts (Fig. 2). Before the impacts, in the 13 to 16 July time period, the 58.4-nm signal was quite low (but significant) at a level of 2.9 ± 0.9 R. After the impacts of what were thought to be the larger comet fragments, a marked increase in the helium emissions occurred. The strongest signals (actually only about 8 to 12 photons detected per 13-min observation interval) follow about 2 to 4 hours after several of the major impacts. The low count rates observed with EUVE require that we use Poisson statistics to estimate their significance (*14*). The error bars for each measurement in Fig. 2 show the 90% confidence limits for the number of counts from Jupiter, given a mean foreground of 3.57 ± 0.05 counts for each 13-min period (determined by averaging 260,000 s of foreground data taken by EUVE between 13 July and 12 August). In this analysis, the most significant event occurred after the impact of the Q1 fragment. The brightnesses corresponding to the 90% confidence limit count rates for this event were 25 to 70 R, about 8 to 25 times the average brightness of Jupiter just before the impacts. Notable brightenings were also seen (although with considerably less significance) after some of the other fragment impacts. For instance, there is a less than 5% chance that the He I 58.4-nm brightness of Jupiter after the F, G, and K events was less than 12, 7, and 10 R, respectively (Fig. 2).

It is interesting to examine whether these large brightnesses can be reasonably ascribed to resonant scattering of sunlight. Using a resonance-line radiative-transfer code (*15*),

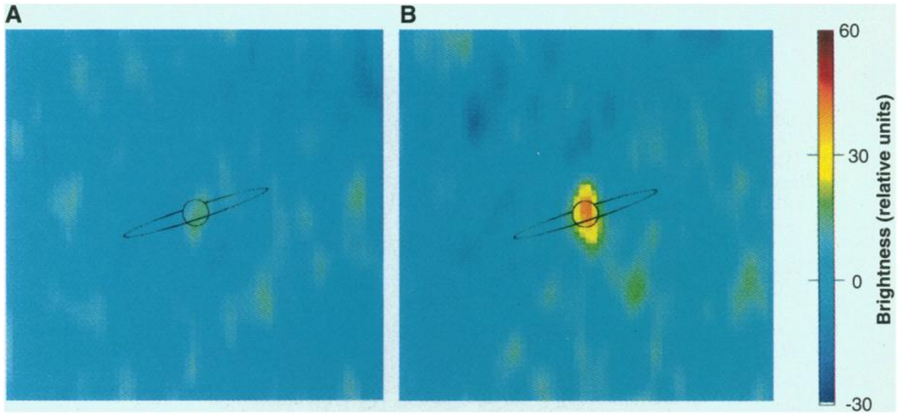

Fig. 1. Images of Jupiter at 58.4 nm obtained by EUVE (**A**) before (13 to 16 July 1994) and (**B**) during (17 to 21 July 1994) the impacts of comet Shoemaker-Levy 9. The brightness of Jupiter at 58.4 nm during the impacts (averaged over 15.1 hours of data) increased by 3.4 times over its value before the impacts (averaged over 16.5 hours of data). A schematic illustration of the disk of Jupiter and the orbit of Io are overplotted at the expected position and orientation of Jupiter. The data have been smoothed by the EUVE point spread function to increase the signal-to-noise ratio. The relatively bright geocoronal 58.4-nm foreground emissions [which fill the aperture of EUVE's telescope and collimator, resulting in a broad (about 2-nm FWHM) terrestrial feature] have been subtracted.

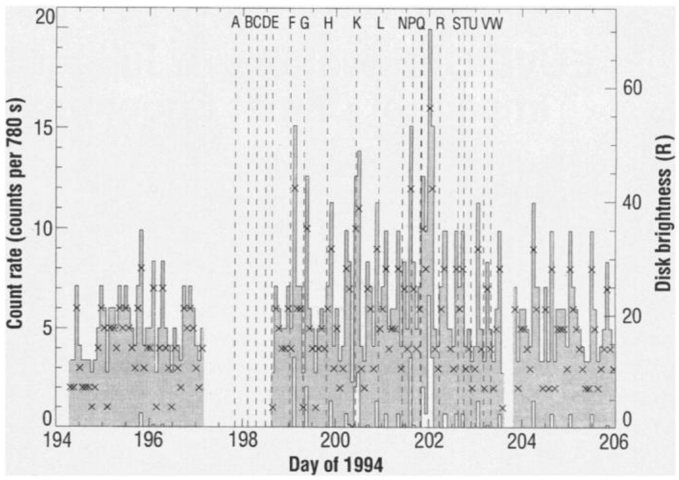

Fig. 2. Light curve of the EUVE He I 58.4-nm signal observed throughout the comet impact period. The data (shown as crosses) represent the actual counts detected for each EUVE orbit during the last 13 min that Jupiter was observable (chosen to minimize the geocoronal foreground). The shaded region gives the 90% confidence level range for the source (that is, Jupiter) count rates given a mean foreground level of 3.57 ± 0.05 counts per interval. The scale on the right converts these source count rates to brightnesses, assuming that the emitting region is the size of the disk of Jupiter. The times of the fragment impacts are indicated as dashed vertical lines. Several significant brightening events are seen to follow 2 to 4 hours after the larger impacts, most notably after the Q1 fragment impact.

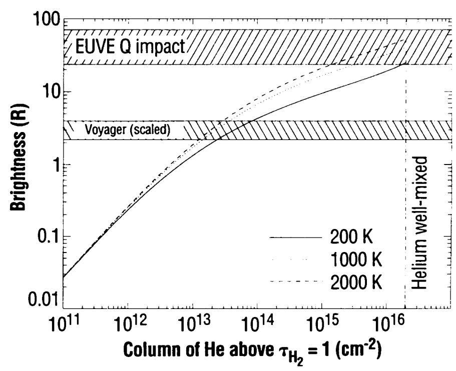

Fig. 3. Model curve-of-growth for the He I 58.4-nm emission on Jupiter. Calculated with an isothermal model atmosphere at temperatures of 200, 1000, and 2000 K, the vertical emission brightness for normal incidence sunlight is shown as a function of the column abundance of He atoms above the level at which the absorption optical depth of 58.4-nm radiation by H_2 reaches unity (τ_{H_2} = 1). The 90% confidence level range of the brightness observed after the Q1 fragment impact is indicated, as is the brightness observed by the Voyager UVS instruments (scaled by a factor of 0.65 to account for the expected difference in solar flux between the time of the Voyager measurements and the comet impact). The brightenings observed after the impacts of the larger fragments are consistent with the expected brightness caused by resonant scattering of sunlight from the high-altitude remains of the impact plumes. The limiting column abundance of about 2 × 10^{16} atoms per square centimeter is reached when the helium in the upper atmosphere is well mixed at its tropospheric level of f_{He} = 11%.

we simulated the subsolar brightness of Jupiter at 58.4 nm for a variety of model atmospheres, producing characteristic curves-of-growth (Fig. 3). The solar flux at 1 astronomical unit (AU) was assumed to be 2.5 × 10^9 photons cm^{-2} s^{-1} with a Gaussian line shape and a full width at half maximum (FWHM) of 0.012 nm (*16*). The observed emission brightness occurs on the logarithmic part of the curve-of-growth, so that the He I 58.4-nm brightness observed after the Q1 impact would require an increase in the column abundance of helium over the entire disk of Jupiter by about two orders of magnitude or more over the levels inferred for the upper atmosphere from the Voyager UVS observations. Although this seems to be an extreme requirement, we can illustrate its plausibility as follows. The plume from a 3-km-wide impactor has been calculated to contain an atmospheric mass of roughly 15% of the impactor mass above an altitude of 400 km, at which level its velocity is about 20 km s^{-1} (*17*). Assuming a deep atmosphere mixing ratio of f_{He} = 11%, the amount of helium in such a plume would be roughly 6 × 10^{36} atoms (assuming a 3-km-diameter impactor with a density of 0.1 g cm^{-3}). Spread over the surface of Jupiter, the column density of helium would be about 10^{16} atoms per square centimeter, which would put the expected brightness within the limits imposed by the EUVE observations. At 20 km s^{-1}, the plume could conceivably spread laterally by a distance equal to the radius of Jupiter (71,400 km) in about 1 hour. Although we do not expect the plume to completely envelop the planet, it seems reasonable that a substantial fraction of the observable half of the planet would be covered with well-mixed columns of hydrogen and helium on the time scale required by the EUVE observations because the impact sites rotate into near sub-Earth position about 2 to 3 hours after they are created. We thus conclude that EUVE observations of transient brightenings of 58.4-nm radiation from Jupiter after the impacts of the Q1 and several other fragments of comet Shoemaker-Levy 9 are consistent with resonantly scattered sunlight from the high-altitude atmospheric remains of plumes created by the impact events.

Other possible sources of He I 58.4-nm emissions include electron impact excitation and recombination of He^+ ions, assuming that energetic electrons or large abundances of He^+ ions are generated by the impacts. To investigate the possible contribution from these sources, we constructed light curves for He I 53.7-nm emission (corresponding to a resonance transition from the next highest energy level of helium above the state responsible for the 58.4-nm emission) and emission at 50.4 nm (corresponding to emission expected during electron recombination with He^+ ions). Neither of these light curves show statistically significant events. Models of resonant scattering of the solar He I 53.7-nm line lead to brightnesses of <4.5 R in the most generous case (well-mixed He at 2000 K), which is consistent with the lack of significant events in the 53.7-nm light curve. The data do not rule out the possibility of a minor contribution by electron impact excitation of He or radiative recombination of He^+ ions after the large impacts. However, on the basis of measured values of the electron impact excitation cross sections for 58.4-, 53.7-, and 50.4-nm (Rydberg) emissions (*18*), the upper limit for electron impact contributions to the 58.4-nm signal is <16 R. Radiative recombination is also improbable (*2*). Thus, we believe that the most plausible explanation for the enhanced He I 58.4-nm emissions is resonantly scattered sunlight from a column of helium in Jupiter's upper atmosphere that was temporarily increased across much of the planet's disk.

REFERENCES AND NOTES

1. R. W. Carlson and D. L. Judge, *Planet. Space Sci.* **19**, 327 (1971).
2. The contribution from photoelectron impact excitation of neutral helium was estimated at 0.03 R [J. J. Olivero, J. N. Bass, A. E. S. Green, *J. Geophys. Res.* **78**, 2812 (1973)]. The contribution from radiative recombination of He^+ ions is also very low because of the inefficiency of the radiative recombination process compared with other reactions available to ionospheric He^+ ions.
3. The line-integrated solar flux at 1 AU varies over the solar cycle by a factor of roughly 3, from about 1.5 × 10^9 photons cm^{-2} s^{-1} at solar minimum to about 4.2 × 10^9 photons cm^{-2} s^{-1} at solar maximum, and the variation over a 27-day solar rotation at solar maximum is about ±20% [W. K. Tobiska, *J. Atmos. Terr. Phys.* **53**, 1005 (1991)].
4. The much brighter UV resonance line of atomic hydrogen at 121.6 nm (Lyman α) is less useful than the He I 58.4-nm line for these studies because the chemistry of H in Jupiter's upper atmosphere is not adequately understood. Instead, we can use models of vertical mixing based on He I 58.4-nm observations in analyses of Lyman α observations to provide constraints on the sources and sinks of atomic hydrogen in the homopause region.
5. The rayleigh (R) is a unit of surface brightness equivalent to an intensity of 10^6 photons cm^{-2} s^{-1} per 4π steradians. The flux received at a detector from a source with brightness *B* (in rayleighs) is $F = 10^6 B\omega/4\pi$ (in photons per square centimeter per second), where ω is the solid angle of the source as seen from the detector (in steradians).
6. R. W. Carlson and D. L. Judge, *J. Geophys. Res.* **79**, 3623 (1974).
7. J. C. McConnell, B. R. Sandel, A. L. Broadfoot, *Planet. Space Sci.* **29**, 283 (1981). The brightnesses quoted are from a recent reanalysis of the Voyager 1 and 2 He I 58.4-nm data [R. J. Vervack Jr., B. R. Sandel, G. R. Gladstone, J. C. McConnell, C. D. Parkinson, *Icarus* **114**, 163 (1995)]. The solar flux at 1 AU of He I 58.4-nm radiation during the times of the Voyager 1 and 2 flybys are estimated to have been 4.0 × 10^9 and 3.5 × 10^9 photons cm^{-2} s^{-1}, respectively.
8. S. Bowyer and R. F. Malina, in *Extreme Ultraviolet Astronomy*, R. F. Malina and S. Bowyer, Eds. (Pergamon, New York, 1991), pp. 397–408; A. Miller, "EUVE Guest Observer Handbook," *NASA Res. Announce. 94-OSS-13* (Office of Space Science, National Aeronautics and Space Administration, Washington, DC, 1994), appendix G.
9. The two longer wavelength spectrographs are collimated in the dispersion direction to 20 arc min to minimize diffuse Earth airglow contamination. The spectrograph gratings have variable line spacings to maintain a sharp focus while dispersing the EUV photons. The on-axis angular resolution is about 24 arc sec for point sources at 58.4 nm, and individual pixels span 4.4 arc sec in the spatial direction. The point source spectral resolution at 58.4 nm is 0.2 nm. After broadband filtering to exclude contaminating non-EUV emissions, the dispersed and focused EUV photons are collected by microchannel plate detectors that record the two-dimensional location and arrival time of each photon. For an extended object having an emission line spectrum (such as Jupiter or the Io torus), the detectors record a series of monochromatic images of the object. The resulting spatial-spectral image is commonly referred to as an "overlappogram."
10. The corrections to a Jupiter-fixed frame of reference were made by software provided by the EUVE Guest Observer staff, along with a detailed ephemeris for Jupiter generated with the SPICE-NAIF software made available by the Jet Propulsion Laboratory [C. Acton, unpublished material].
11. D. T. Hall *et al.*, *Astrophys. J.* **426**, L51 (1994).
12. The overhead geocoronal He I 58.4-nm brightness measured by an EUV spectrometer on the P78 spacecraft in 1979 (at an altitude of 600 km) varied from about 500 R in the subsolar region [S. Chakrabarti, F. Paresce, S. Bowyer, R. Kimble, *J. Geophys. Res.* **88**, 4898 (1983)] to about 2 R in the antisolar region [S. Chakrabarti, R. Kimble, S. Bowyer, *ibid.* **89**, 5660 (1984)].
13. P. Jelinsky, J. V. Vallerga, J. Edelstein, *Astrophys. J.* **442**, 653 (1995).
14. R. P. Kraft, D. N. Burrows, J. A. Nousek, *ibid.* **374**, 344 (1991).
15. G. R. Gladstone, *J. Geophys. Res.* **93**, 14623 (1988).
16. The line-integrated solar flux was estimated from (*3*). The line shape for the solar He I 58.4 nm line was estimated from C. Y. R. Wu and H. S. Ogawa, *ibid.* **91**, 9957 (1986).
17. M. B. Boslough, D. A. Crawford, A. C. Robinson, T. G. Trucano, *Geophys. Res. Lett.* **21**, 1555 (1994); D. A. Crawford, M. B. Boslough, T. G. Trucano, A. C. Robinson, *Int. J. Impact Eng.*, in press.
18. The cross sections for the emission of 58.4-, 53.7-, and 50.4-nm (principal quantum number $n > 5$) radiation through impact excitation of He by 200-eV electrons are 7.94 × 10^{-18}, 2.05 × 10^{-18}, and 1.11 × 10^{-18} cm^2, respectively [D. E. Shemansky, J. M. Ajello, D. T. Hall, B. Franklin, *Astrophys. J.* **296**, 774 (1985)]. If the observed 53.7-nm signal of about 4 R or less were due entirely to electron impact, the corresponding signal at 58.4 nm would be at most about 16 R (although probably less because of the larger absorption cross section of hydrogen at 58.4 nm compared with that at 53.7 nm).

19. We would like to thank the EUVE team at the University of California, Berkeley, for their support in making the EUV observations of Jupiter before and during the comet impacts. In particular, we would like to thank G. Bevan, J. Hinchman, P. Jelinsky, A. Keith, T. Kilsdonk, F. Kronberg, R. Malina, J. McDonald, D. Meriwether, E. Olson, J. Vallerga, and G. Wong for their tremendous efforts in acquiring and processing the data in nearly real time. We would also like to acknowledge the other members of our EUVE proposal—F. Bagenal, J. Clarke, P. Feldman, M. McGrath, W. Moos, N. Schneider, D. Shemansky, and D. Strobel—and especially the other EUVE Jupiter–Shoemaker-Levy 9 campaigners—F. Herbert, R. Lieu, and N. Thomas—for their assistance and cooperation in planning the observations. The comments of an anonymous referee were very useful. The support of NASA grants NAG5-2651 to Southwest Research Institute, NAG5-2622 to Johns Hopkins University, and NAS5-30180 to the Center for Extreme Ultraviolet Astrophysics at the University of California at Berkeley are gratefully acknowledged.

18 October 1994; accepted 15 March 1995